Analysis of 2-Carbon-11-Thymidine Blood Metabolites in PET Imaging

Anthony F. Shields, David Mankoff, Michael M. Graham, Minna Zheng, Susan M. Kozawa, Jeanne M. Link and Kenneth A. Krohn

Department of Medicine and Imaging Research Laboratory, Department of Radiology, University of Washington; and Seattle Department of Veterans Affairs Medical Center, Seattle, Washington

Carbon-11-thymidine labeled in the ring-2 position was used with PET to image tumor and tissue proliferation. Since thymidine is rapidly degraded in the body, one must consider the generation of metabolites to fully interpret the PET data. **Methods:** We have measured the blood time-activity curves of thymidine and its metabolites in arterial blood samples. Blood was processed to obtain three input curves, including the total activity, the activity with CO_2 removed and the fraction of CO_2-free activity in intact thymidine (% Tdr). **Results:** We found that CO_2 reached a plateau of 65% (±12%) of total blood activity by 11 min after injection. When a 1-min infusion of labeled thymidine is used, the time to 50% degradation to thymine and metabolites other than CO_2 (measured in acidified samples by HPLC) was 2.9 ± 0.6 min. We fit the results of the blood metabolism with a compartmental model. We found that we could accurately determine the %Tdr curve with as few as three measured points with an root mean square (RMS) error of 2% in the integrated curve, compared to the curve using all blood samples (mean of seven samples per patient). The integral of thymidine blood activity serves as the input to thymidine models, so similar errors could be expected in calculations of DNA synthetic rates. We found that the determination of CO_2 could be accomplished with as few as five samples, with an RMS error of 4% in plateau $\%CO_2$ value. **Conclusion:** While it is essential to take metabolites into account when interpreting results obtained with ^{11}C-thymidine, the reproducibility of these degradation curves may allow the use of a limited number of samples to measure the catabolic products of thymidine. These data from the blood, along with tissue kinetic models, are needed to calculate DNA synthetic rates.

Key Words: thymidine; carbon dioxide; PET; cancer

J Nucl Med 1996; 37:290–296

Carbon-11-thymidine and PET are being used to detect tumors and measure tumor proliferation in vivo (*1–3*). PET obtains images of all the radioactive chemical species retained within a tissue. Thymidine labeled with ^{11}C in the ring-2 position is rapidly degraded in vivo to thymine, CO_2 and other compounds. Therefore, to model the uptake of thymidine and use it to quantitate tumor proliferation, one must take into account the kinetics and distribution of these metabolites. The first step in such a process is measuring the time course of the metabolites in the blood. These studies were undertaken to determine the best method of measuring these metabolites and to mathematically model their generation.

MATERIALS AND METHODS

Radiochemistry

Carbon-11-thymidine labeled in the ring-2 position was prepared immediately prior to use according to a modification of the method of Vander Borght et al. (*4*). The radiochemical purity of HPLC isolated material was 98% ± 2% (except for one study with a value of 85%). The entire preparation of ^{11}C-thymidine from $^{11}CO_2$ required 70–80 min and is done robotically (*5*). As we gained experience with the synthesis, the amount of carrier urea used decreased, resulting in higher specific activities. The amount of ^{11}C-thymidine injected ranged from 211 to 685 MBq (5.7–18.5 mCi) and the specific activity was 0.13–13 GBq/μmole (3.5–350 Ci/mmole) at the time of injection. The amount of thymidine injected ranged from 0.013 to 2.4 μmole.

Subjects

We evaluated blood samples from 17 studies of 14 patients. This included five patients with nonsmall-cell lung cancer, two with small-cell lung cancer, three with sarcoma and one each with colon cancer, undifferentiated neoplasia, sarcoidosis and a volunteer with heart disease. Two patients with small-cell lung cancer and one with sarcoma were studied before and a week into chemotherapy. The subjects were all male and ranged in age from 23 to 70 yr (mean 54 yr) and weighed from 60 to 112 kg (mean 81 kg). The medical records of the subjects were reviewed and information from the blood counts, serum chemistries and liver function tests were recorded. Since platelets are the major source of thymidine phosphorylase in the body (*6–8*), we also recorded the platelet volume as well as the platelet count.

As part of PET imaging studies, catheters were placed in a radial artery for blood sampling and an intravenous catheter was placed in the opposite arm or a leg for thymidine infusion. The ^{11}C-thymidine was diluted to 20 ml with physiologic saline and infused intravenously over 60 sec using a Harvard syringe pump. Imaging was done over 60 min after injection. All study protocols had been approved by institutional Human Subject and Radiation Safety Committees, and all subjects gave informed consent.

Blood Sampling

Blood samples (1.0 ml) were drawn from the arterial line using an automated blood sampler (*9*) into heparinized test tubes containing, in most cases, approximately 40,000 cpm of ^{3}H-thymidine (1.5–2.6 GBq/μmole) to act as an internal standard for thymidine degradation that occurred during processing. For each study, the radiochemical purity was >99% as assayed by HPLC (*10*). Sampling was performed at 10-sec intervals over the first minute after injection, then 20-sec intervals over the second min, then at 3, 4, 5, 7, 9, 11, 13, 15, 18, 21, 24, 27, 30, 35, 40, 45, 50, 55 and 60 min. Aliquots of blood were immediately transferred to test tubes for fixation of CO_2 (0.2 ml) for removal of CO_2, (0.2 ml), and for HPLC (0.4 ml). The test tube for CO_2 fixation (TOTAL) contained 0.8 ml of 0.5 N NaOH and was rapidly capped to retain all labeled CO_2 as bicarbonate. The test tube used for CO_2 removal (ACID) contained 0.6 ml of isopropanol, and this was followed by the addition of 0.2 ml of 0.5 N HCl (*11*). The sample was vortexed after each addition to prevent gelation. Nitrogen gas was then bubbled through each acidified sample for 10 min while incubated in a water bath at 60°C before assaying for radioactivity. Tests demonstrated that this technique removed >99% of $^{11}CO_2$ and

Received Nov. 22, 1994; revision accepted May 15, 1995.

For correspondence or reprints contact: Anthony Shields, MD, Wayne State University, Harper Hospital, 534 Hudson, 3990 John R St., Detroit, MI 48201.

bicarbonate from the blood (*11*). The CO_2 activity was calculated by subtracting the CO_2-free ACID blood activity from the TOTAL activity.

The 0.4-ml blood sample for HPLC was placed in a 1.5-ml Eppendorf tube with 0.8 ml of 0.5 *M* perchloric acid. Included in the tube was 2,000 cpm of ^3H-H_2O (629 MBq/mole; NEN) and 4,000 cpm of ^{14}C-thymine as internal standards. The thymine was produced from ^{14}C-thymidine (1.85–2.22 GBq/mmole) by cleavage with *E. coli* thymidine phosphorylase. The radiochemical purity of the HPLC isolated material was >99%. After vortexing the sample was centrifuged for 2 min at 14,000 rpm and the supernatant was removed and filtered through a 0.45μ Acrodisc LC13 PVDF (Gelman Sciences, Ann Arbor, MI). The sample (0.75 ml) was analyzed on a reverse-phase column 250 × 4.6 mm with a guard column of LC-18 pellicular packing (50 × 4.6 mm). The mobile phase was 10% methanol and water. An HPLC miniPump VS (LDC/MiltonRoy, Riviera Beach, FL) was run at 2.5 ml/min. Beginning 0.5 min after injection, fractions were collected every 15 sec for 5 min. Between 3 and 10 specimens were analyzed for each patient. All NaOH-treated, acid-treated and HPLC samples were then measured by gamma spectrometry using a 10-detector scintillation system. Results were decay-corrected to the time of injection. HPLC samples subsequently were mixed with 6 ml of Scint-AXF (Packard, Meridien, CT) scintillation cocktail to verify the fractions containing the void volume, thymine, and thymidine. The relative ^3H activity in the thymidine and thymine peaks was used to correct for degradation of ^{11}C-thymidine to thymine during processing (average 4%). It should be noted that the rapid HPLC separation used in this study does not separate thymine from dihydrothymine, and a mixture of the two is present in vivo (*12*). This ambiguity in our analysis, however, does not effect the quantitation of the fraction present as thymidine.

Data Analysis of Blood Results

As previously discussed, blood sampling and metabolite analysis result in three sets of data. These include the relatively finely time-sampled measures of the TOTAL and CO_2 free ACID blood activity (in μCi/ml; up to 28 samples per study), as well as more coarsely time-sampled data on the percentage of activity in thymidine (%Tdr) from HPLC analysis of selected acid treated samples. To model the behavior of ^{11}C-thymidine in vivo, the blood time-activity curves for labeled thymidine (Tdr), labeled CO_2 (CO_2), and labeled non-CO_2 metabolites (Metab) are needed as input functions. These are calculated from the raw data as follows:

$$\text{Tdr} = \text{ACID}*(\%\text{Tdr}/100), \qquad \text{Eq. 1}$$

$$\text{Metab} = \text{ACID}(1 - \%\text{Tdr}/100), \qquad \text{Eq. 2}$$

$$CO_2 = \text{TOTAL} - \text{ACID}. \qquad \text{Eq. 3}$$

HPLC is time consuming; thus only a limited number of specimens can be analyzed by HPLC. Because the value of labeled CO_2 requires the subtraction of two measured values, the resulting time-activity curve can be noisy, especially late in the study when blood radioactivity levels are low. With this in mind, we analyzed two characteristic metabolite curves: the %Tdr curve obtained from HPLC analysis and the percentage of labeled CO_2 (%CO_2), given by

$$\%CO_2 = \frac{\text{TOTAL} - \text{ACID}}{\text{TOTAL}}. \qquad \text{Eq. 4}$$

For each type of characteristic curve, analysis was carried out in three steps: First, the characteristic metabolite curves from all studies were pooled to calculate an average curve. Second, simple models were employed to smooth and interpolate the individual metabolite fraction curves. Thirdly, the original data were sub-sampled to examine how the model might allow us to reduce the number of samples required to undergo metabolite analysis. These last two analyses were suggested by the similarity of the characteristic metabolite curves for all patients studied, which led us to investigate the use of constrained curve fitting methods to reduce blood sampling and metabolite analysis requirements. To fit the characteristic metabolite curves, two separate compartmental models were used: one to fit the %Tdr curve and one to fit the %CO_2 curve. The models are intended solely for curve fitting and not as a mathematical description of thymidine kinetics in the blood. The models are detailed in the appendix and highlighted briefly below.

The %Tdr curves were modeled using a five-parameter, three-compartment model with first-order kinetics. The measured ACID curve serves as the input to two blood compartments (blood thymidine and blood non-CO_2 metabolites), while a single tissue compartment represents tissue handling of all labeled species. The model is optimized against the %Tdr data obtained from HPLC analysis, generating a smooth and continuous fit of the %Tdr data (see Appendix for details). To compare the %Tdr curves resulting from application of the model, two characteristic measures were used: (1) the time until 50% of the acidified blood thymidine activity is degraded and (2) the relative integral of intact thymidine blood activity, obtained from multiplying the %Tdr curve times the ACID curve as in Equation 2.

With the aim of decreasing HPLC requirements, we tested the use of a reduced number of HPLC analyses to characterize the %Tdr curve. The patients' original raw %Tdr data sets were sub-sampled to form three sets containing one (at 3 min), two (at 2 and 5 min) or three (at 2, 4 and 7 min) data points. These sets were used in the %Tdr compartmental model, and the resulting interpolated %Tdr curves were compared to those obtained with the full %Tdr data sets. Errors resulting from fitting the subsampled curves are expressed as the worst case and RMS differences in the 50% degradation time (min) and relative integrated thymidine time-activity curve (percent of the integral of the fully-sampled curve). The RMS difference in these curve measures is defined as follows:

$$\text{RMS Difference} = \left(\sum (X_S - X_F)^2/N\right)^{1/2}, \qquad \text{Eq. 5}$$

where X_S is the measure of the sub-sampled curve, X_F is the measure of the fully sampled curve (100% in the case of the relative integrated thymidine activity), and N is the number of patients included in the analysis (=17). This can be thought of as a measure of the average error in the %Tdr curve resulting from using fewer samples and interpolation by the model. The timing of the subsampled data points was chosen based on trials of optimal sample timing with three individual data sets. In patients where these time samples were not available, neighboring time points were used (eight patients). In addition, to test the feasibility of using the average %Tdr curve and no HPLC analysis, each patient's %Tdr curve obtained using all HPLC data points was compared to the average %Tdr curve.

For the %CO_2 curves, another compartmental model was used (see Appendix). The %CO_2 model is a five-parameter, three-compartment model using the TOTAL curve as the input to the blood compartments and is used to generate smooth and interpolated %CO_2 curves. The model is optimized against the %CO_2 data points calculated according to Equation 4. The resulting fitted curves were evaluated by two measures: the average percent CO_2 plateau value from 11 to 60 min and the relative integral CO_2 time-activity curve.

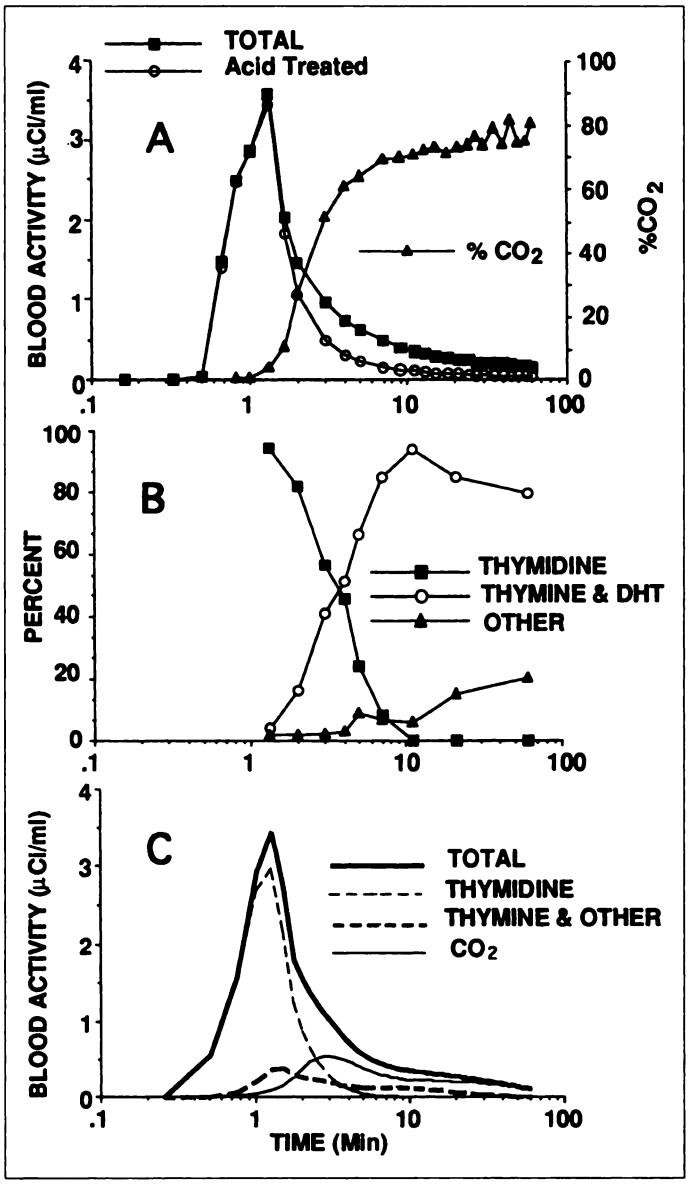

FIGURE 1. Analysis of blood activity in a patient after injection of 2-^{11}C-thymidine. (A) Total blood activity was measured in NaOH fixed blood, and acid treatment was used to remove CO_2. (B) The difference between these samples was used to calculate the percentage in CO_2. (C) HPLC analysis of acidified blood demonstrates the rapid degradation of thymidine to thymine and dihydrothymine (DHT). The time scale is logarithmic to better view the rapid degradation.

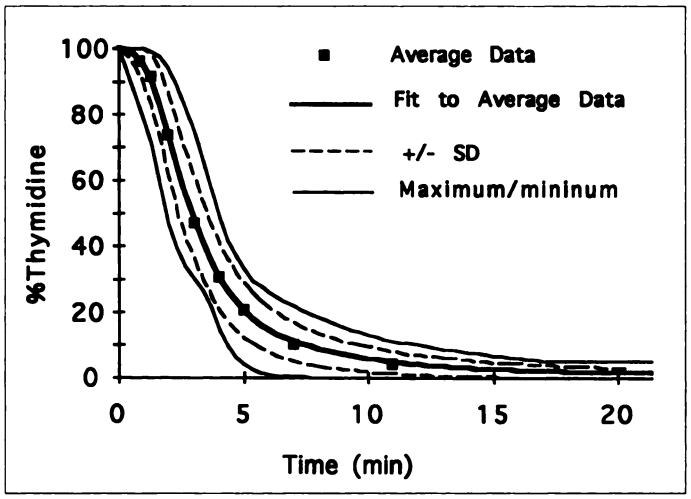

FIGURE 2. Percent of activity in thymidine as measured by HPLC in acid-treated blood. Plot of the average percentage in thymidine at each time point, along with the curve of the average fit and the curves representing ±1 s.d. and maximum and minimum values, determined using the fit curves.

As with the %Tdr data, the $\%CO_2$ data were subsampled to form smaller datasets consisting of five points, a fit was generated, and the resulting $\%CO_2$ curves were compared to the curves obtained from the full dataset. The timing of these samples was optimized by examining data from selected patients; chosen time points were 2, 4, 11, 21 and 40 min. As in the HPLC analysis, in patients where these time samples were not available, neighboring time points were chosen (six patients). In two patients, input TOTAL time points were not available 40 min postinjection. For the purpose of the above analysis, the fit $\%CO_2$ curves were extended, assuming a constant value after 40 min in these cases.

RESULTS

As seen in a typical patient study (Fig. 1), 2-[^{11}C]thymidine is rapidly degraded to thymine and subsequently to CO_2. HPLC analysis demonstrated that by 4 min after injection more activity was in thymine and dihydrothymine than thymidine. As indicated in the Methods section, we did not separate thymine from dihydrothymine; the latter being the principal blood metabolite (*1*). Comparison of the NaOH fixed and acid treated blood showed that by 3 min after injection there was more activity in CO_2 than thymidine and by 8 min approximately 65% of the blood activity was in CO_2. The rapid generation of the labeled thymine and CO_2 demonstrates the need to correct the input function for any kinetic models for the presence of these compounds.

HPLC analysis was performed on 3–10 samples (mean 7) from each patient in the hour after injection. The curve of the percentage of activity in thymidine was fit using the compartmental model for interpolation and smoothing (Fig. 2). On average, the thymidine was 50% degraded by 2.9 min (s.d. = 0.6, range 1.9–4.0). Furthermore, we could find no significant correlation between subject age, weight or surface area and the time to 50% thymidine degradation. We also found no correlation between white blood count, hematocrit, platelet count, platelet count times volume, total bilirubin, SGOT, SGPT or alkaline phosphatase and the time of degradation. The only patient characteristic that correlated with the degradation time was the serum creatinine ($r = 0.67$; $p < 0.005$, range for creatinine 1.0–1.8 mg/dl). The specific activity at the time of injection, or injected mass did not affect the rate of metabolism. The dose of injected activity had a small correlation with degradation time ($r = 0.58$, $p = <0.02$), but this correlation failed to be significant when the Bonferoni correction for multiple paired tests was applied. For the greatest amount of total thymidine injected (2.4 μmole), the maximal blood level of labeled thymidine reached a peak of 0.47 μM at 80 sec after the start of the infusion (20 sec after its completion), then decreased to 0.039 μM by 3 min after the start of infusion. With improvements in the specific activity of the labeled thymidine, more recently injected doses have been lower by more than a factor of 50. The typical native blood level of thymidine is 0.1 μM (*13*). Thus, under most circumstances, we were below this level.

Subsample analysis results for the %Tdr curve are shown in Table 1 and Figure 3. Using the subsampled curves, we calculated the time (min) to 50% degradation and the percentage difference in the relative integrated thymidine time-activity curves. Errors are expressed as the worst case and RMS differences between the subsampled curve and the curve ob-

TABLE 1
Comparison of Percent Thymidine Curve Fitting Using a Limited Number of HPLC Samples (1–3) with Full Sampling Sequence

Measure	Three*	Two*	One*	Average curve
Percent error in integrated TdR activity				
Worst case error (%)	4.7	9.8	9.5	27.2
RMS error (%)	2.0	5.2	5.7	11.5
Time to 50% degradation				
Worst case error (min)	0.6	0.4	1.6	1.0
RMS error (min)	0.2	0.2	0.5	0.6

*Three = three-point fit; two = two-point fit; one = one-point fit, respectively.

tained using all samples. The use of only three HPLC points instead of the full set resulted in an RMS error in the integrated thymidine time-activity curve of only 2% and a worst case error of 5%. These errors increased when fewer points were used in the fit and reached a maximum error of 12% RMS, 27% worst case, when the pooled mean %Tdr curve was used in lieu of HPLC analysis. Use of a limited number of data points resulted in only small changes in the time to 50% degradation and ranged from an RMS error of 0.2 min with a three-point fit, to 0.6 min using the average curve (Table 1).

Similar to our analysis of the HPLC curve we analyzed the generation of CO_2 in the patients. We found the shape of the curve of percent of blood activity in CO_2 ($\%CO_2$) versus time after injection was consistent from patient to patient, with some variability in the plateau $\%CO_2$ value (Fig. 4). This plateau value, calculated as the average fraction of activity in CO_2 between 11 and 60 min had a mean value of 65% (s.d. 13%, range 41%–79%). Subsample analysis (see Table 2) using the $\%CO_2$ measurement from only five time points resulted in only minor errors in the plateau and integrated CO_2 values in comparison to the full set of data (28 samples).

DISCUSSION

While the use of ^{11}C-thymidine offers the opportunity to measure in vivo DNA synthesis, the metabolism of this compound must be taken into account in order to more fully

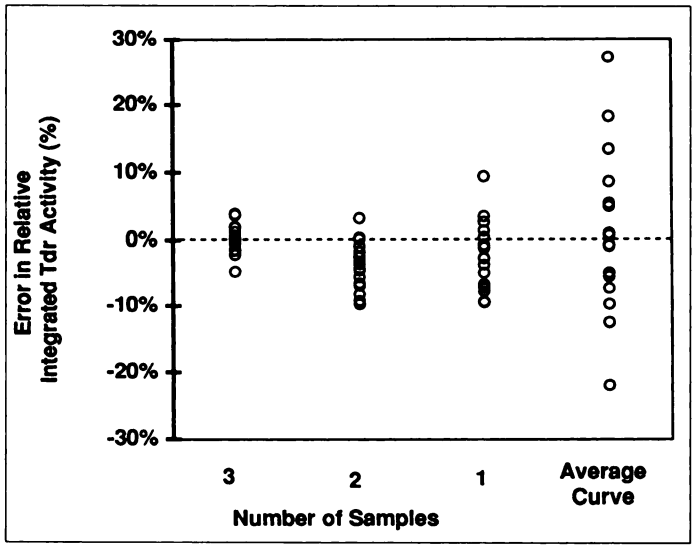

FIGURE 3. Plot of the error in integrated time activity for each patient. This is a comparison of the results obtained using the full data set compared with the fits using a limited number of samples or the average curve.

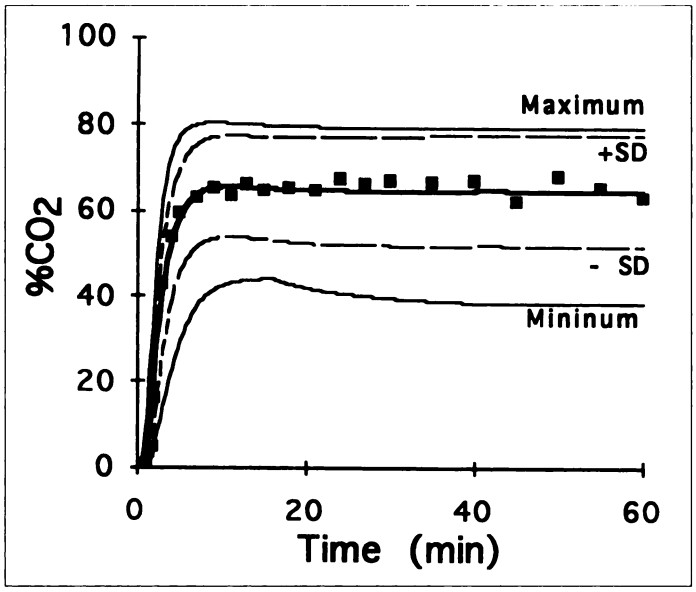

FIGURE 4. Percentage of total blood activity in CO_2. The plot shows average percentage in CO_2 at each time point, along with the curve of the average fit and the curves representing ±1 s.d. and maximum and minimum values, determined using the fit curves.

interpret the PET images (*11,14*). Through a series of studies we have demonstrated that the retention of labeled thymidine in tissues is dependent upon its incorporation into DNA, that endogenous synthesis and local reutilization are predictable and that one must take into account the distribution of metabolites (*10,11,15,16*). This latter problem has led us to the routine measurement of arterial blood samples and an HPLC analysis of the metabolites present in the blood. The synthesis of 2-^{11}C-thymidine, as developed by Vander Borght (*4*), offers some improvements over methyl-^{11}C-thymidine, since it generates fewer metabolites. Nevertheless, the degradation of thymidine to thymine and labeled CO_2 must still be taken into account.

In this study, we sought to measure the generation of metabolites and to determine the number of specimens required to provide reliable estimates of thymidine and metabolite blood activity over time. The difficulty of analyzing multiple HPLC samples and the determination of blood activity in CO_2 would preclude a complete quantitative analysis of thymidine PET images under routine clinical circumstances. If one could utilize total blood time-activity curves along with standard metabolic curves and a limited number of blood samples, then wider use with quantitation would be more practical. Our models have demonstrated the ability to fit the characteristic metabolite curves and to allow more coarsely time-sampled metabolite analysis without significant loss of accuracy in metabolite quantitation. One could measure the total blood activity with fine time sampling and measure the %Tdr and $\%CO_2$ on a small number of samples, three and five, respectively. The $\%CO_2$

TABLE 2
Comparison of CO_2 Curve Fitting Using a Limited Number of Blood Samples (Five) with Full Sampling Sequence

Measure	Five-point fit	Average curve
Percent CO_2 plateau value		
Worst case error (%)	7.5	23.4
RMS error (%)	3.5	11.5
Error (%) in integral of percent CO_2 curve		
Worst case error (%)	8.2	58.1
RMS error (%)	3.2	21.9

TABLE 3
Starting Values and Limits for Model Parameters
(Units for Parameters Are per Minute)

Parameter	Starting value	Minimum	Maximum
	%Tdr Model		
k1	0.4	0	2
k2	0.1	0	2
k3	0.5	0	2
k4	0.5	0	2
k5	0.05	0	2
	$\%CO_2$ Model		
k1	0.5	0	1
k2	0.5	0	1
k3	0.5	0	2
k4	0.5	0	1
k5	0.5	0	1

curve could then be fit directly using the model and the %Tdr curve fit using the CO_2-free activity curve obtained from the total measurements and the fit $\%CO_2$ curves.

Ultimately, we wish to calculate the thymidine incorporation rate (TIR) from the tissue time-activity curves generated from the PET images and from the blood thymidine and metabolite input curves. Our results demonstrated that the input blood time-activity curves necessary could be generated using a limited number of blood samples. We would expect that the errors in the integrated thymidine blood activity from limited sampling would cause approximately proportional errors in the TIR estimate. This is supported by our preliminary modeling of thymidine metabolism (*17*). The effect of errors in the $\%CO_2$ determination are less clear, but would likely be less significant than errors in the %Tdr curve determinations.

In reviewing our results, one must remember that they only apply to the metabolism of 2-^{11}C-thymidine. Although methyl-^{11}C-thymidine is also degraded to thymine and dihydrothymine, subsequent metabolic steps result in the generation of little CO_2. Furthermore, our results were generated using a 60-sec infusion. While we could find no correlation between the metabolism of thymidine and its specific activity or the injected mass, one might find different results if the specific activity was lower than the levels used here. It was only in our early patients, when a larger amount of carrier urea was used in the synthesis, did we approach the native level of thymidine (about 0.1 μM) for a short time. We are now injecting 50-fold less thymidine by mass.

Given the reproducibility of our results, one might be tempted to use the average HPLC curve that we have generated, but this resulted in errors has high as 27.2% in the integrated thymidine activity. It is also important to remember the other limitations of the average HPLC curve. These studies were only performed on men, but we do not expect that women would metabolize thymidine differently. None of our patients had markedly abnormal blood counts or severe liver, renal or other metabolic problems. For example, it might be expected that patients with severe liver dysfunction might generate CO_2 more slowly. The slower degradation of thymidine seen with increasing creatinine, may reflect decreased clearance and degradation of thymidine by the kidney. Further studies in patients with severe renal and hepatic failure may be useful in exploring these issues. Patients smaller or larger than the group we studied here might have altered metabolism of thymidine, and no children were included in our study. In all of these situations, it would be important to obtain at least a limited number of HPLC samples to validate the degradation curve. Based on our results, we think that three samples obtained at 2, 4 and 7 min after injection would probably be sufficient.

Ultimately, one would wish to do quantitative imaging with thymidine without the need for an arterial line and with a limited number of venous blood samples. In such a situation, the input function may be obtained from measuring the time-activity curve over the heart or a great vessel. Such an approach clearly needs to be validated. One may be able to use the average HPLC curve as given above, which would greatly simplify the performance of the PET study. To limit the errors, HPLC measurements might be done on a limited number of samples taken from a vein, but this will need to be directly tested in further studies. While the percentage of activity in CO_2 reaches a plateau early in the study, the plateau level appears to vary significantly from patient to patient. It will be of interest to determine if two or three venous samples obtained 10 min postinjection are sufficient for reasonable quantitation.

CONCLUSION

Whereas thymidine is rapidly degraded in vivo, the generation of its metabolites is very predictable. With the use of appropriate kinetic models, one may be able to perform limited blood sampling and analysis and yet attain reasonably accurate quantitative measurements. Further studies are clearly needed to define the best way to utilize a limited amount of blood data to attain sufficient accuracy in measurements of tumor growth and response to therapy.

APPENDIX

The intention of the models is twofold: (a) to smooth and interpolate the metabolite data obtained from analysis of the blood samples and (b) to predict the form of the characteristic metabolite curves so that the curves can be defined using fewer analysis points, as in the sub-sample analysis. Initially, simple curve-fitting methods such as multi-exponential fits and simple two-compartment models were tried; however, these methods did not work well in all patients and specifically had trouble in the case of the %Tdr curve, where the shoulder in the early portion of the curve could not be fit well with these simple approaches. Subsequently, a more complex model served as the starting point for each type of metabolite curve. This model contained a blood and tissue compartment for each class of labeled chemical species. The models were then empirically simplified to the minimum number of compartments and parameters necessary to obtain good fits of the curves for each of the patients. For all patients, the models were required to converge to a reasonable solution from the common parameter starting values and ranges listed in Table 3. More complex models than those described below were insufficiently constrained to accurately and reliably predict the metabolite curves from a more limited number of sample points. Our approach was thus to use a model complex enough to fit the characteristic curves of our 17 patients, yet simple enough to provide sufficient constraint to be able to predict curves from a reduced number of data points. Two separate models were used to describe the %Tdr curve and the $\%CO_2$ curve.

For the %Tdr model, the CO_2 free activity serves as the input to a model describing the degradation of thymidine to thymine, dihydrothymine, and beta-ureidoisobutyric acid (metabolite class). Since the %Tdr measurement uses CO_2-free activity, labeled CO_2 is outside the bounds of the model and therefore not included. The %Tdr, as a function of time after injection, is calculated from the model's prediction of the activity in the blood thymidine and blood

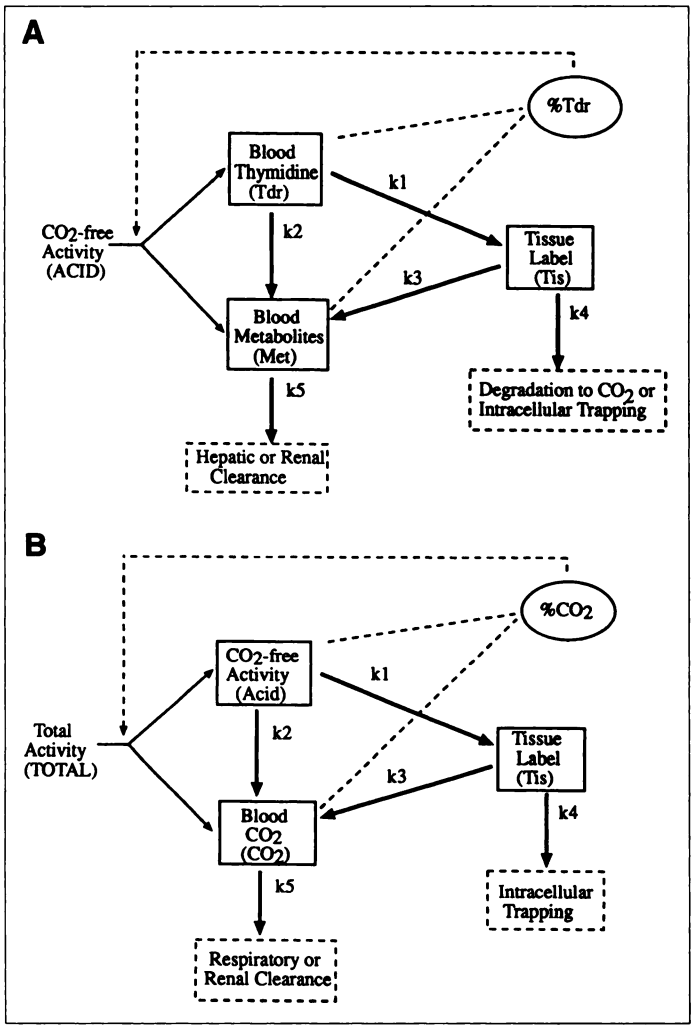

FIGURE 5. Diagram of models used for fitting (A) percent thymidine (%Tdr) curve and (B) percent CO_2 (%CO_2) curve.

non-CO_2 metabolite compartments. The %Tdr model is described by the following equations (Fig. 5A):

$$dTdr/dt = -(k1 + k2)*(\%Tdr/100)*ACID, \quad \text{Eq. A1}$$

$$dMet/dt = -k5*(1 - \%Tdr/100)*ACID + k2*Tdr + k3*Tis, \quad \text{Eq. A2}$$

$$dTis/dt = -(k3 + k4)*Tis + k1*(\%Tdr/100)*ACID, \quad \text{Eq. A3}$$

$$\%Tdr = Tdr/(Tdr + Met)*100, \quad \text{Eq. A4}$$

where Tdr is the blood thymidine compartment activity (μCi/ml), Tis is the tissue compartment activity (μCi/ml), Met is the blood metabolite compartment activity (μCi/ml) and ACID is the Measured CO_2-free blood activity (μCi/ml).

In the model, the measured CO_2-free blood activity (ACID) serves as the input function and is divided between the two blood compartments according to the values for %Tdr (initial value 100%). Only degradation and uptake (and not synthesis of thymidine) is allowed. Linear kinetics between compartments is assumed. Thymidine degradation in the blood is described by the parameter k2. Thymidine transfer into tissue and degradation plus transport back to the blood are described by k1 and k3, respectively. Metabolite clearance from the CO_2-free blood compartment is given by the parameter k5. Both tissue degradation of thymidine to CO_2 (in the liver for example) and incorporation of thymidine into macromolecules results in the removal of thymidine or CO_2-free metabolites from potential access to the blood. These processes are described by k4. In our original formulation of the models, efflux from the tissue compartment to the blood thymidine compartment and influx from the blood metabolite compartment to the tissue compartment were included, however inclusion of these parameters did not improve the fit to the data. Therefore, these were eliminated in the final form of the model. All parameters have units min^{-1}.

A similar testing process led to the formulation of a model for the %CO_2 curve. Again, a three-compartment model was required to fit the data accurately, and it provided enough constraint to provide accurate predictions of the %CO_2 curves in sub-sample analysis. The following equations describe the model (Fig. 5B):

$$dAcid/dt = -(k1 + k2)*(1 - \%CO2/100)*TOTAL, \quad \text{Eq. A5}$$

$$dCO_2/dt = -k5*(\%CO2/100)*TOTAL + k2*Acid + k3*Tis, \quad \text{Eq. A6}$$

$$dTis/dt = -(k3 + k4)*Tis + k1*(1 - \%CO2/100)*TOTAL, \quad \text{Eq. A7}$$

$$\%CO_2 = CO_2/(Acid + CO_2)*100, \quad \text{Eq. A8}$$

where Acid is the CO_2-free blood compartment activity (μCi/ml); (modeled as opposed to measured); Tis is the tissue compartment activity (μCi/ml); CO_2 is the blood CO_2 compartment activity (μCi/ml); and TOTAL is the measured total blood activity, including CO_2 (μCi/ml).

In this case, the total blood activity (TOTAL) serves as the input, which is divided between two compartments: the blood CO_2-free activity compartment and the blood labeled CO_2 compartment, according to the %CO_2 value (initial value 0). As in the %Tdr model, all labeled species in tissues are considered to be in a single compartment. In the case of CO_2 generation, most of the degradation will take place in tissue organs such as the liver. Transport into the tissue and release of CO_2 back to the blood are described by parameters k1 and k3, respectively. For completeness, the parameter k2 (degradation to CO_2 in the blood) is included. Clearance of CO_2 from the blood and tissue are represented by k5 and k4, respectively. All parameters have units min^{-1}.

Both models were implemented on Macintosh workstations using the Bopt (*18*) modeling environment. Optimization of the model was performed using the Marquardt-Levenberg nonlinear optimizer (*19*). Starting values and limits for the models' parameters are listed in Table 3.

ACKNOWLEDGMENTS

Supported in part by grants CA 42045 and CA 39566 from the National Cancer Institute and by the Medical Research Service of the Department of Veterans Affairs.

REFERENCES

1. Eijkeren ME, Schryver AD, Goethals P, et al. Measurement of short term ^{11}C-thymidine activity in human head and neck tumours using positron emission tomography (PET). *Acta Oncol* 1992;31:539–543.
2. Martiat P, Ferrant A, Labar D, et al. In vivo measurement of carbon-11 thymidine uptake in non-Hodgkin's lymphoma using positron emission tomography. *J Nucl Med* 1988;29:1633–1637.
3. Vander Borght T, Pauwels S, Lambotte L, et al. Brain tumor imaging with PET and 2-[carbon-11]thymidine. *J Nucl Med* 1994;35:974–982.
4. Vander Borght T, Labar D, Pauwels S, Lambotte L. Production of [2-^{11}C]thymidine for quantification of cellular proliferation with PET. *Appl Radiat Isotopes* 1991;42:103–104.
5. Courter JH, Link JM, Krohn KA. Automation of the synthesis of [2-carbon-11]thymidine. In: Weinreich R, ed. *Proceeding of the Fourth Workshop on Targetry and Target Chemistry*. Paul Scherrer Institute; Villigen, Switzerland: 1992:210–214.
6. Shaw T, Smillie RH, Miller AE, MacPhee DG. The role of blood platelets in nucleoside metabolism: regulation of platelet thymidine phosphorylase. *Mutat Res* 1988;200:117–131.

7. Shaw T, Smillie RH, MacPhee DG. The role of blood platelets in nucleoside metabolism: assay, cellular location and significance of thymidine phosphorylase in human blood. *Mutat Res* 1988;200:99–116.
8. Usuki K, Norberg L, Larsson E, et al. Localization of platelet-derived endothelial cell growth factor in human placenta and purification of an alternatively processed form. *Cell Regulation* 1990;1:577–596.
9. Graham MM, Lewellen BL. High-speed automated discrete blood sampling for positron emission tomography. *J Nucl Med* 1993;34:1357–1360.
10. Shields AF, Lim K, Grierson J, Link J, Krohn KA. Utilization of labeled thymidine in DNA synthesis: studies for PET. *J Nucl Med* 1990;31:337–342.
11. Shields AF, Graham MM, Kozawa SM, et al. Contribution of labeled carbon dioxide to PET imaging of carbon-11-labeled compounds. *J Nucl Med* 1992;33:581–584.
12. Cleaver JE. Thymidine metabolism and cell kinetics. *Frontiers Biol* 1967;6:43–100.
13. Nottebrock H, Then R. Thymidine concentrations in serum and urine of different animal species and man. *Biochem Pharmacol* 1977;26:2175–2179.
14. Vander Borght TM, Lambotte LE, Pauwels SA, Dive CC. Uptake of thymidine labeled on carbon 2: a potential indicator of liver regeneration by positron emission tomography. *Hepatology* 1990;12:113–118.
15. Quackenbush RC, Shields AF. Local re-utilization of thymidine in normal mouse tissues as measured with iododeoxyuridine. *Cell Tissue Kinetics* 1988;21:381–387.
16. Shields AF, Coonrod DV, Quackenbush RC, Crowley JJ. Cellular sources of thymidine nucleotides: Studies for PET. *J Nucl Med* 1987;28:1435–1440.
17. Mankoff DA, Shields AF, Lee TT, Graham MM. Tracer kinetic model for quantitative imaging of thymidine utilization using ^{11}C-thymidine and PET [Abstract]. *J Nucl Med* 1994;35:138P.
18. Graham MM. Parameter optimization programs for positron emission tomography data analysis. *Ann Nucl Med* 1993;7:S42–S43.
19. Press WH, Flannery BP, Teukolsky SA, Vetterling WT. *Numerical recipes in Pascal: the art of scientific programming*. New York: Cambridge University Press; 1989. 572–580.

FDG-PET Evaluation of Therapeutic Effects on VX2 Liver Tumor

Natsuo Oya, Yasushi Nagata, Nagara Tamaki, Takehisa Takagi, Rumi Murata, Yasuhiro Magata, Mitsuyuki Abe and Junji Konishi
Departments of Radiology and Nuclear Medicine, Faculty of Medicine, Kyoto University, Kyoto, Japan

Transplanted VX2 liver tumor in the rabbit is an experimental liver tumor model in which ^{18}F-2-fluoro-2-deoxy-D-glucose (FDG) accumulates to a 3.5-fold level that surrounds normal liver tissue. In this study, changes in FDG uptake were assessed in this liver tumor model after transcatheter arterial embolization (TAE) and radiotherapy. **Methods:** Fifteen rabbits bearing VX2 liver tumors were treated with TAE with gelatin sponges 1 day before the FDG study, and 18 rabbits received local irradiation with electron beams at a dose of 12–36 Gy 1–10 days before the FDG study. In the FDG study, serial arterial blood sampling was performed to determine arterial input (AI), and 1 hr after tracer injection, normal liver tissue and tumor tissue were excised to measure radioactivity. The tumor FDG level per AI and the tumor-to-normal liver ratio were assessed. Dynamic PET images were obtained in 20 of the 46 rabbits. **Results:** Tumor FDG uptake was significantly decreased 1 day after TAE (from 3.54 to 0.83 in the tumor-to-normal liver ratio) and 5 days after 30 Gy of irradiation (from 3.54 to 1.28). The decrease in tumor FDG uptake was dose-dependent, especially in the relatively low dose range (12–24 Gy). The untreated tumors could be clearly distinguished from the surrounding normal liver tissue, while the embolized tumors or the irradiated tumors were not clearly delineated. Histological analysis showed that the decrease in tumor FDG after treatment agreed well with the decrease in number of viable tumor cells. **Conclusion:** The VX2 liver tumor is an appropriate experimental tumor model for evaluating the change in FDG uptake in various therapeutic modalities. Moreover, the therapeutic effects can be assessed 1 day after TAE and 5 days after irradiation. Further clinical trials for the early evaluation of therapeutic effects on liver tumors using FDG-PET are warranted.

Key Words: fluorine-18-fluorodeoxyglucose; VX2 tumor; transcatheter arterial embolization; radiotherapy

J Nucl Med 1996; 37:296–302

Many experimental and clinical studies have shown increased uptake of ^{18}F-2-fluoro-2-deoxy-D-glucose (FDG) in malignant tumors with increased glucose utilization (*1–7*). In terms of clinical use, metabolic imaging of tumors by FDG-PET is useful in differentiating malignant tumor from benign disease (*8–10*), assessing the degree of differentiation (*11–15*) and detecting recurrences (*10,16*). In addition, several studies have suggested the usefulness of FDG-PET for evaluating therapeutic effects. Most of these clinical studies indicated that FDG uptake in tumors decreases after radiotherapy (*17–22*), chemotherapy (*18*) and transcatheter arterial embolization (TAE) (*23*). Some of these studies suggest that the prognosis could be predicted by the decrease in tumor FDG uptake (*18,21,22*).

Also, decreased FDG uptake following radiotherapy or chemotherapy has been demonstrated in mouse and rat experimental tumor models (*24–27*). Transplanted VX2 tumor in the rabbit is an experimental tumor model in which FDG accumulates to levels several-fold those in normal organs (*2–4*). In our previous study, VX2 tumors transplanted in the rabbit liver were evaluated by FDG-PET (*5*). In the present study, the change in FDG uptake in the transplanted VX2 liver tumor was assessed after TAE and radiotherapy to determine the usefulness of FDG-PET in this model for evaluating the effects of therapy.

MATERIALS AND METHODS

Animals and Tumors

Male Japanese white rabbits (weighing 2–4 kg) were used in this study. Rabbits were anesthetized with 25 mg/kg b.w. sodium pentobarbital, and a midline abdominal incision was made. Two-to-six blocks of VX2 tumor tissue containing approximately 4–10 $\times 10^5$ VX2 cells were transplanted directly into each rabbit's liver (*5,28*). Forty-six rabbits with VX2 liver tumors over 2 cm in diameter 3–4 wk after transplantation were used in the following experiments. Twenty-one of these rabbits had multiple liver tumors and/or nonhepatic tumors (e.g., tumors in overlying muscular layer or peritoneum).

FDG

Fluorine-18 was produced by the ^{20}Ne(d, α)^{18}F nuclear reaction using an ultracompact cyclotron. Fluorine-18-FDG was then synthesized by the acetylhypofluorite method of Shiue et al. (*29*) with slight modifications. The specific activity of the [^{18}F]FDG thus obtained was 143 to 204 MBq/mg and the radiochemical purity was over 95% as assessed by HPLC (eluent, CH_3CN:H_2O = 85:15).

Received Dec. 27, 1994; revision accepted Jul. 29, 1995.
For correspondence or reprints contact: Natsuo Oya, MD, Department of Radiology, Kyoto University Hospital, 54 Kawahara-cho, Shogoin, Sakyo-ku, Kyoto 606, Japan.